SAND2016-10574R

Enhanced Surveillance Annual Report for FY16

SAND2016-???? (DC: Tony Geller)

September 25th, 2016

Modeling Manufacturing Impacts on Aging and Reliability of Polyurethane Foams

Kevin Long, Christine Roberts, Lisa Mondy, Melissa Soehnel, Kyle Johnson, Henry Lorenzo, and Rekha Rao (PI)

Sandia National Laboratories
Albuquerque, NM 87185

Abstract

Polyurethane is a complex multiphase material that evolves from a viscous liquid to a system of percolating bubbles, which are created via a CO_2 generating reaction. The continuous phase polymerizes to a solid during the foaming process generating heat. Foams introduced into a mold increase their volume up to tenfold, and the dynamics of the expansion process may lead to voids and will produce gradients in density and degree of polymerization. These inhomogeneities can lead to structural stability issues upon aging. For instance, structural components in weapon systems have been shown to change shape as they age depending on their molding history, which can threaten critical tolerances. The purpose of this project is to develop a Cradle-to-Grave multiphysics model, which allows us to predict the material properties of foam from its birth through aging in the stockpile, where its dimensional stability is important.

Introduction

We propose to develop a physics-based computational model, informed by careful experiments, to understand polyurethane expansion and curing with the goals of predicting density and improving foam structural models. A model predicting foam filling and curing within a mold has been developed; this model serves as the initial condition for a subsequent model for stress relaxation and dimensional changes during polyurethane foam aging. A series of experiments were developed in FY15 to obtain validation data for the model. These include polyurethane cure in a simple geometry, foam expansion in a commercial instrument (FOAMAT), and long term aging of a horseshoe shaped foam geometry. In FY15, we completed an initial model framework and determined many of the parameters needed to characterize the nonlinear viscoelastic model. In FY16, we worked to finalize the post-gel curing behavior and to determine the evolving modulus during cure. Once this was completed, rigorous comparisons between the model and the experimental data were the focus. From this work, we have concluded that several mechanisms occur after manufacturing that result in shape change. These include bubble depressurization, water uptake, and post-manufacturing curing chemistry. A forth-coming report will document this effort [Long et al., 2016b].

Below we have summarized the four deliverables for the project in FY16 and discussed the work associated with the deliverables and reference documentation where available.

In the first quarter, we worked to "Re-parameterize kinetic model for curing reactions based on improved IR data. Identify other areas of improvement necessary to capture post-gelation kinetics including vitrification for solid stresses." We determined that a significant component of the kinetics was the foaming reaction, which led to density predictions necessary for the solid deformation analysis. A new foaming model was completed, which used a nucleation term having both a time-scale and a nucleation time. The kinetics and nucleation terms can be seen in equation (1.1).

$$
\begin{aligned}
\frac{dC_{H_2O}}{dt} &= -Nk_{H_2O}C_{H_2O}{}^{n} \\
\frac{dC_{CO_2}}{dt} &= +Nk_{H_2O}C_{H_2O}{}^{n} \\
N &= 0.5\left\{1+\tanh\left(\frac{t-t_{nucleation}}{t_{scale}}\right)\right\}
\end{aligned}
\tag{1.1}
$$

Figure 1 shows the water concentration for PMDI-10 structural foam as a function of time for 4 different temperature, compared to the experimental data. Note the good correlation between model and data at all temperatures.

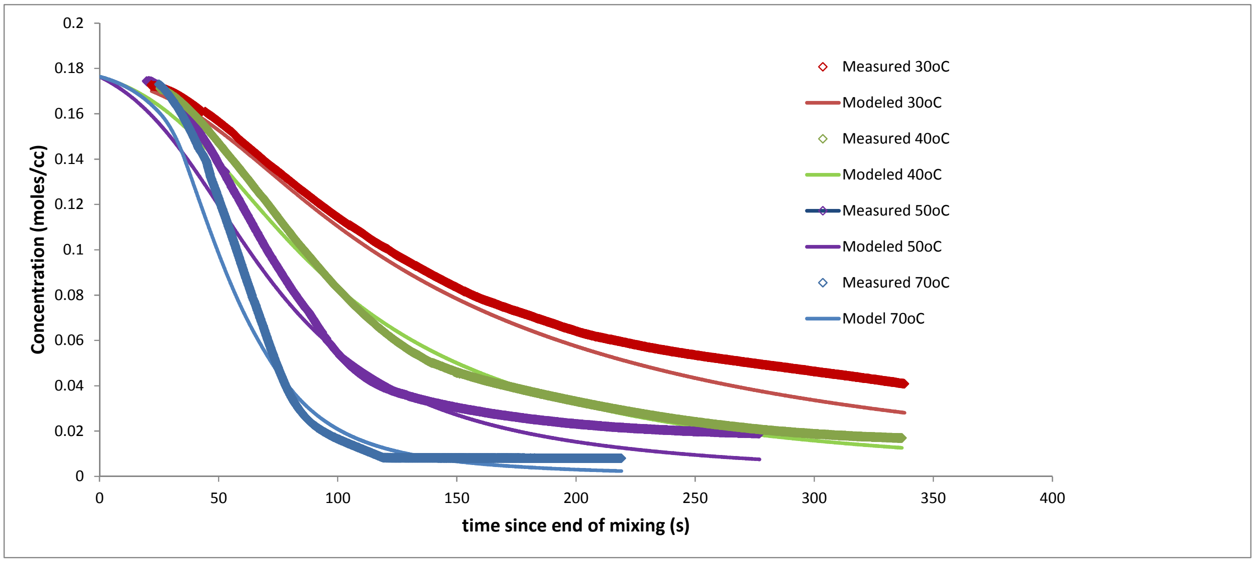

Figure 1. Water concentration for the model compared to data for BKC 44306 PMDI-10 foam at an oven temperature of 30°C, 40°C, 50°C and 70°C.

If we plot the rate data and model, we see the complexity of the water reaction. The reaction rate increases, reaches a maxima and then slowly decreases to zero. Without the nucleation time, we would not be able to capture the non-monotonic behavior of the rate.

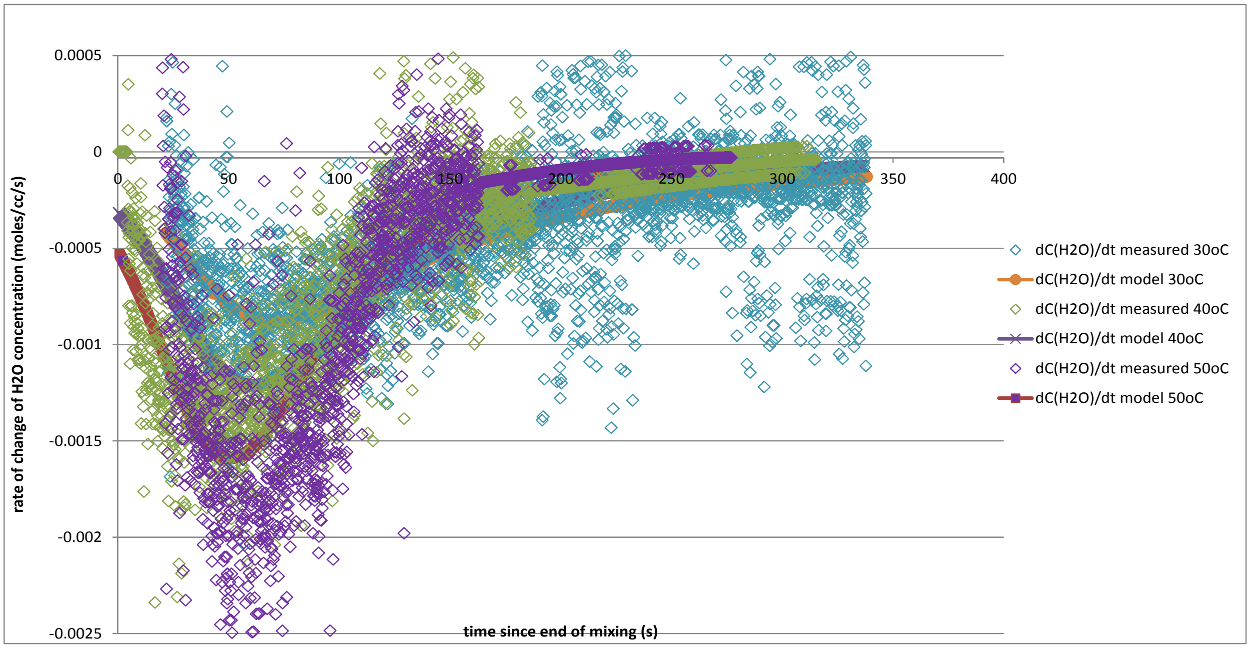

Figure 2. Comparing rate of water depletion predictions to data for PMDI-10 foam at an oven temperature of 30°C, 40°C, 50°C and 70°C.

Predictions of density using a nucleation time of 40s and a time scale of 20s compared to measured density with time in the channel for various temperatures are shown in Figure 3.

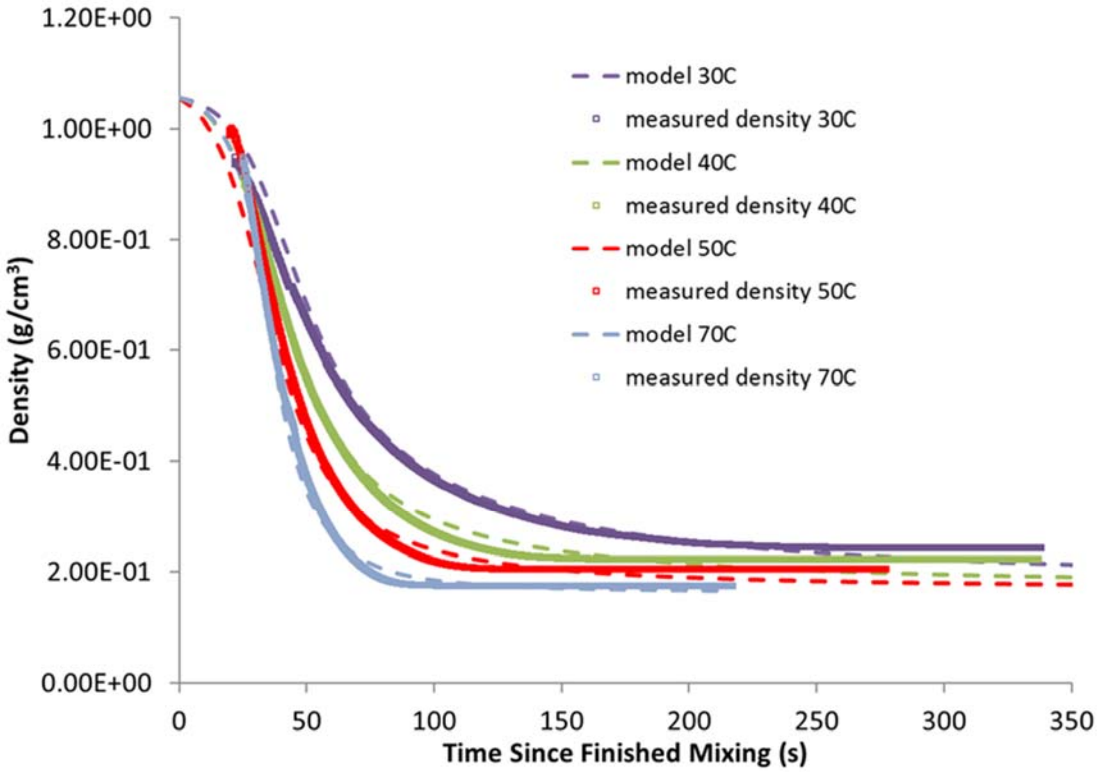

Figure 3 Predictions of density using a nucleation time of 40s compared to measured density with time in the channel for several temperatures. For 70°C, the model uses the Arrhenius form with temperature variations, whereas the other comparisons are made for the nominal temperature of the mold.

Figure 3 shows a comparison of the kinetic predictions to the density data. The data assumes that the density in each isothermal experiment is uniform in space but evolves over time. In reality, we believe that even small-scale, mostly isothermal, experiments will have density gradients including skin effects near walls and gradients associated with the advection of the foam front. This has been seen from post-test x-ray computed tomography (CT) of the fully cured foam, though the x-ray CT technique is too slow relative to the rate of the reactions to give information about the evolving density.

The polymerization kinetics were also refitted and an improved evolving glass transition temperature was parameterized. We have documented this work in a journal article submitted to AICHE Journal, which looks promising for acceptance once the reviewer's comments are addressed [Rao et al., 2016].

In the second quarter, we worked to "develop validated foam filling model for horseshoe geometry using flow visualization data to provide initial conditions for nonlinear viscoelastic stress model." We have developed a foam filling model for PMDI structural foam. This model was used to study filling in a horseshoe geometry shown in the included Figure 4. The top row shows the experimental filling profile. The middle row shows the results from the simulation. The bottom row compares the density predicted by the simulation and the density found from X-Ray CT experiments. It was found that the fluid viscosity was higher than expected in the experiment and the material no longer leveled, but instead kept its initial hemispherical shape. This was important to match for the simulation. The density predictions match qualitatively, but are much more dramatic in the CT data. We are working on developing a more predictive density model, based on a bubble-scale approach. The filling, polymerization, and density predictions are used to provide initial conditions for nonlinear viscoelastic stress model. With the stress model, we can look at the manufacturing stresses after the release from the mold and the aging of the part. This work was documented in a March ES News Note.

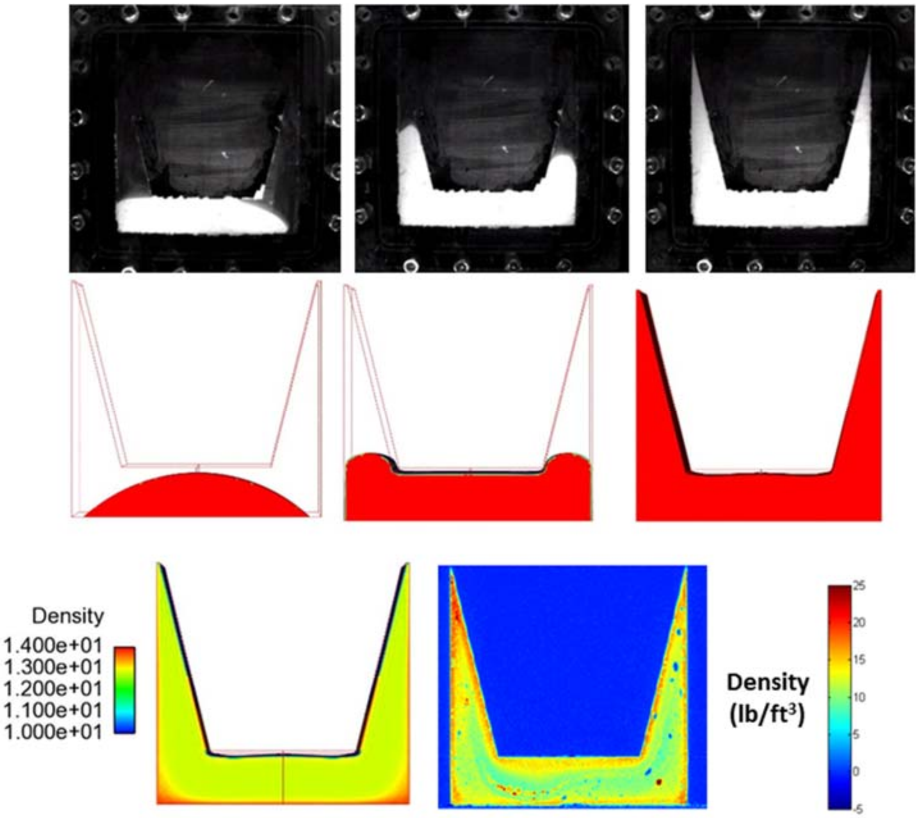

Figure 4. Frames capturing the filling of a staple-shaped mold with foam (top), model predictions of the front location (middle), and (bottom) comparison of model predictions of final density (left) to X-ray CT image (right).

In the third quarter, we worked to "develop model for foam filling, cure, and aging of foam in pop-off geometry. Measure evolving modulus during polymerization for dry polyurethane using a rheometer and DMA." We worked to obtain new data first, since our preliminary data from the previous FY did not have all the parameters we needed for the model such as mass injected and final volume and density. New experiments were designed and carefully carried out by Melissa Soehnel.

The new pop-off tube data were compared to the Sierra/Aria model. The pop-off test is a test developed over 10 years ago by Mark Stavig and company to look at stresses during cure. Material is poured into a pre-heated (40C) cylinder, and, as it cures, the material volume changes, deflecting a thin disk on the bottom. The deflection is recorded by a strain gauge. The experiments are done with free-rising foams because of the sensitivity of the strain gauge. Comparisons of numerical predictions to original data obtained last year revealed that the predicted temperature was very sensitive to the measurement location, and the older experiment only measured temperature at one location. The newer experiments include many more thermocouples at various heights and radial depths for measurements in rising foam (Figure 5). The resulting part has a diameter of 1 inch and a height that depends on the mass injected and the density of the final foam.

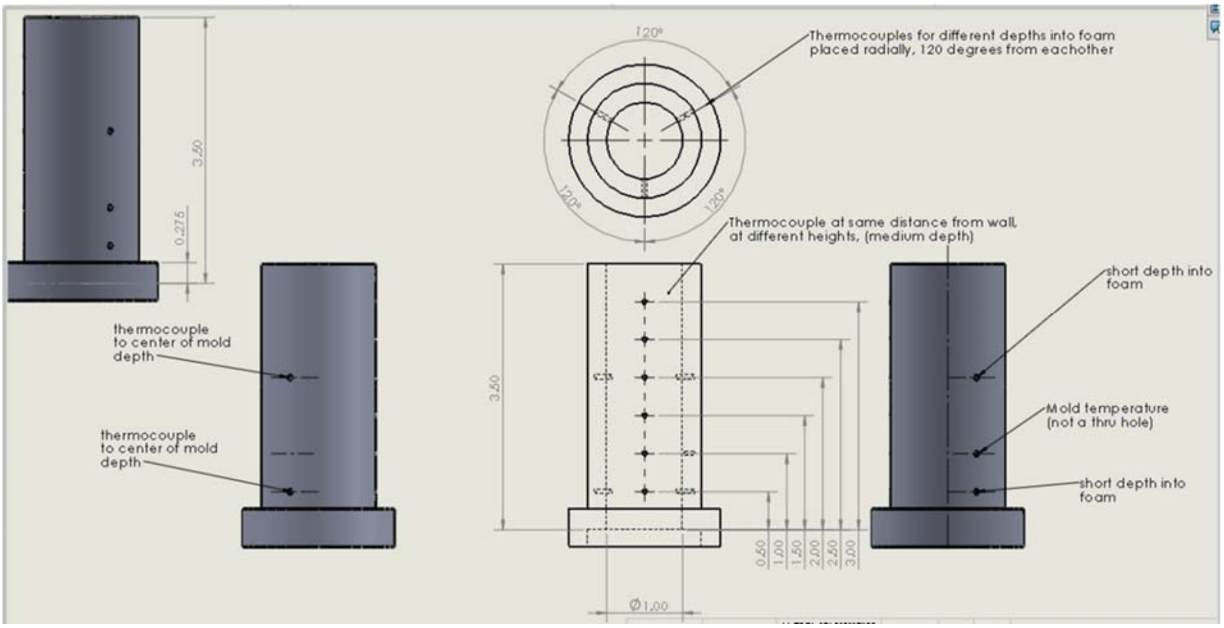

Figure 5. Dimensions of the pop-off tube and location of thermocouples

First we wanted to understand the kinetics of the exothermic reaction and the thermal stress behavior of the polyurethane without bubbles. Our first test showed that the “dry” kit that is supposed to produce no CO_2 had absorbed water, because we ended up with a foam with density 0.59 g/cc (36.9 pcf). Subsequent drying of the kit and a repeat experiment resulted in material with density 0.89 g/cc (55.6 pcf). That density is in line with the expected porosity simply due to air being incorporated during the mixing process.

We ran Sierra/Aria calculations to compare temperature predictions from the kinetics model to the temperatures in the 0.59 g/cc test. The data below show the temperatures and the strain during this first test (Figure 6). The height of the final piece is 1.6 inches, so the thermocouples above that height reflect the air temperature above the polymer. First, looking at the dimensionless strain (the change in length normalized by the initial length), one can see clear evidence of cure shrinkage as the strain gauge goes into compression before transitioning to the oven (where the temperature increases to 120^{o}C). Unfortunately, we have not had time to compare the strain to the coupled flow/structural Sierra/Adagio model. Looking at the temperatures, one sees that the center of the material (e.g. the purple line at a location of the 0.5-inch centerline and a height of 0.5 inch) exotherms to almost the final oven temperature then cools before putting the part in the oven after 10 minutes.

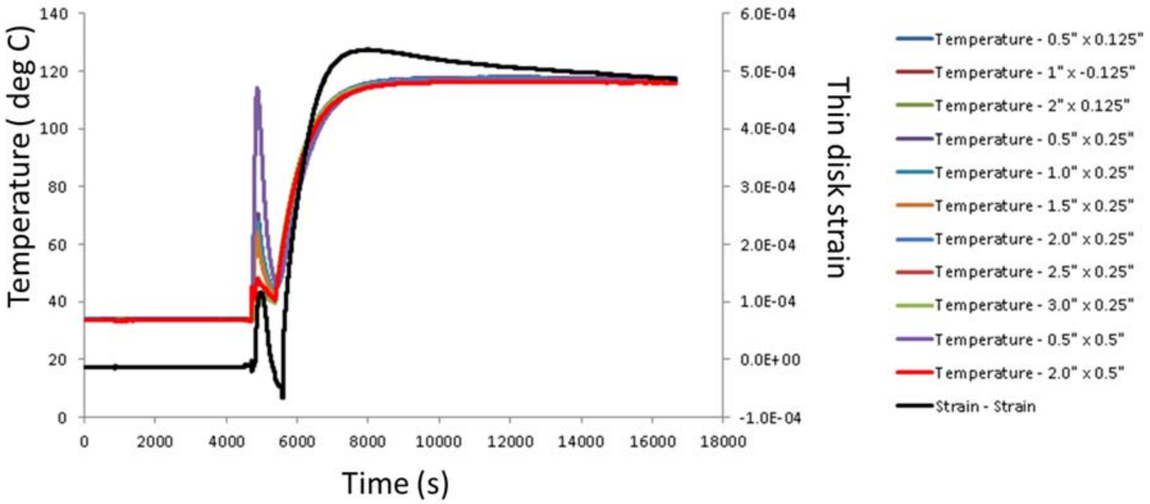

Figure 6. Data from pop-off tube experiment with PMDI-10 dried to produce a density of 36.9 pcf (not from over packing)

Figure 7 shows an expanded section of the data during the filling and early cure, when the cure kinetics are dominating the temperature, and the Aria predictions for the center thermocouple. In doing a careful comparison, we realized that the mesh geometry was slightly different than the actual produced part. A new mesh is being made. The bottom boundary condition is assumed adiabatic in the results below because the apparatus has a large stainless steel ring underneath the thin disk, with some trapped air that discourages heat transfer (Figure 8). The new mesh will better capture the geometry of the mold as well, allowing more accurate heat transfer predictions.

The times were slightly off in the figure, and we may need a more careful match between the cure state at the model zero time and the experiment. The model seems to require a larger heat of reaction than the value used. We plan to go back and get the pedigree of that value and repeat DSC measurements if necessary. Once we have addressed these concerns, we will go back and compare the kinetics model with newer data, as well as look at the mechanical model predictions compared to strain.

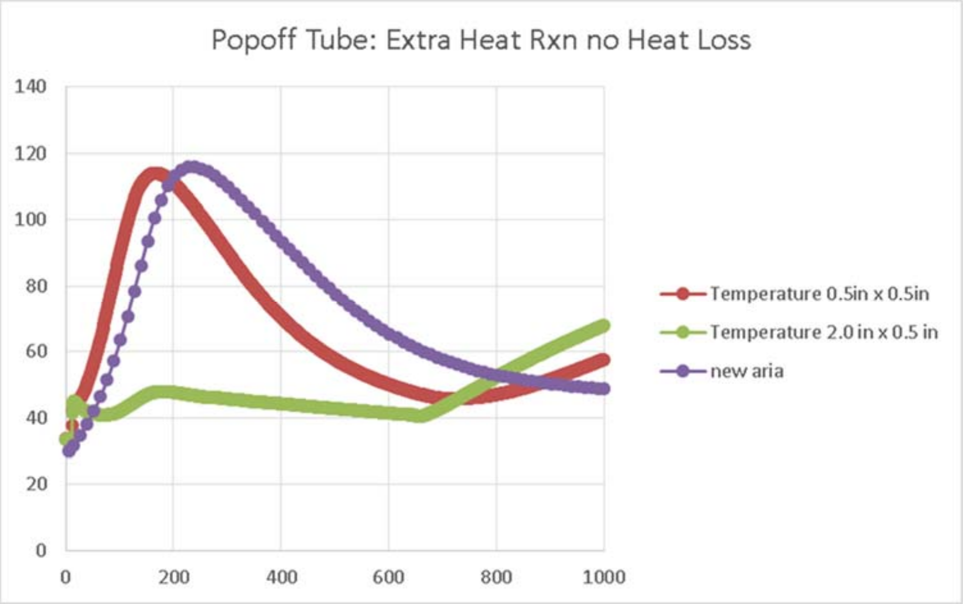

Figure 7. Aria predictions with adiabatic boundary conditions and higher heat of reaction than measured with DSC.

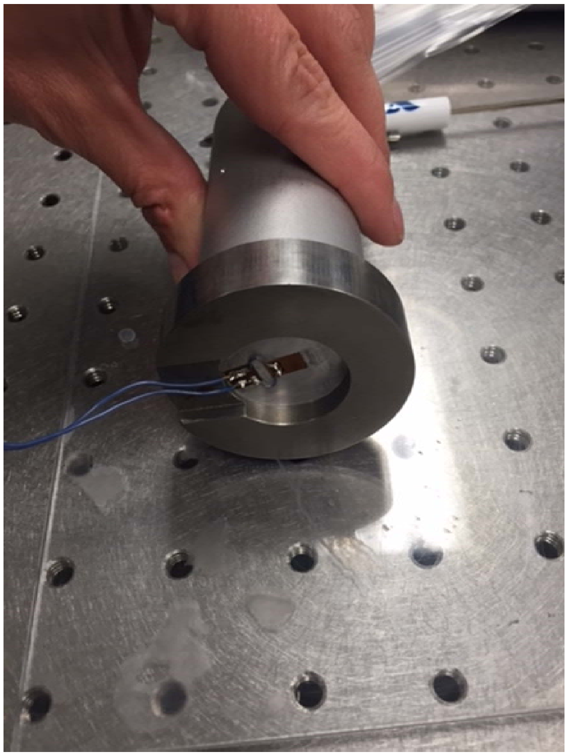

Figure 8. Photo of the bottom of the pop-off tube apparatus, showing the strain gauge and the heavy stainless steel support.

We also collected data on the compressive modulus of the foam as a function of density, to parameterize the solid model. The data are seen in Figure 9.

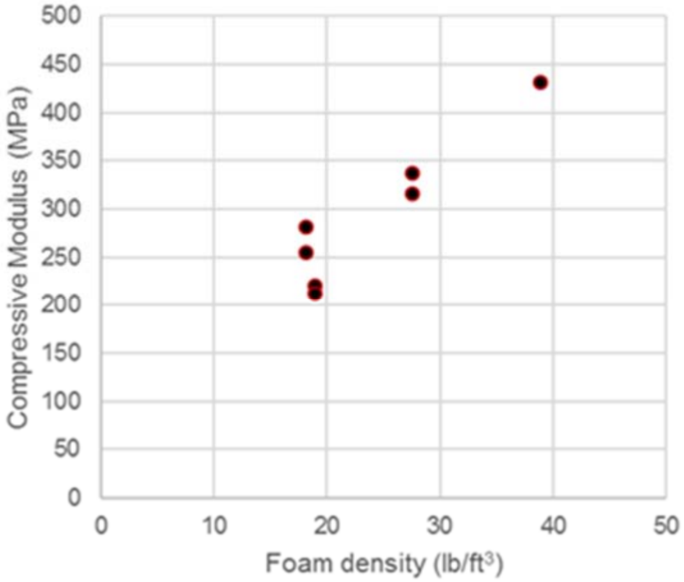

Figure 9. Compressive modulus as a function of foam density.

In the fourth quarter, we worked to "Validate shrinkage and stress relaxation model for horseshoe geometry against experimental data." Triplicate specimens were foamed in the horseshoe mold with good reproducibility of the temperature and pressure profiles. As expected, the base of the staple, which is reached by foam first and is the thickest part of the geometry, reaches the highest temperatures (90^{o}C peak temperature). A slight temperature rise is also observed at the foam tips (50^{o}C). Gauge pressures were observed up to 14 psig at the mold walls; pressures and temperatures are predicted to be higher internally to the sample. X-ray CT images (Figure 10(c)) identify large bubbles that are primarily located in the two upright arms. A dense skin reaching over 20 pcf is also observed at the mold walls as in the front image. Coalescence and formation of large bubbles has been observed previously in regions of high shear in other experiments. A greater packing fraction for this foam would reduce these defects.

Finite element simulations were performed on this geometry from the room temperature state onward using the X-ray CT density. We used the peak measured pressure, ~14 psig, from Figure 10, and applied it uniformly to the part though likely the internal initial gauge pressures are much higher and are functions of density. Typical glassy polymer matrix elastic constants were used ($G \sim 1 \text{ GPa}, \quad \nu \sim 0.4$). We simulated a uniform decay of the gauge pressure and fixed the collections of nodes corresponding to the bolts at the specimen center from the experiment. Similar measurements of dimension change at the waist and 80% along the staple tip were extracted. We found that warpage was an order of magnitude or more lower than experiments, likely a result of too simple an initial gauge pressure variation or too low of a value. We found that predicted warpage was very sensitive to that initial pressure. Qualitatively, the simulations are useful in that they show large regions tend to warp uniformly, but in thin regions, warpage varies spatially. The final warped shapes of the mid-section and front are shown in Figure 10(d).

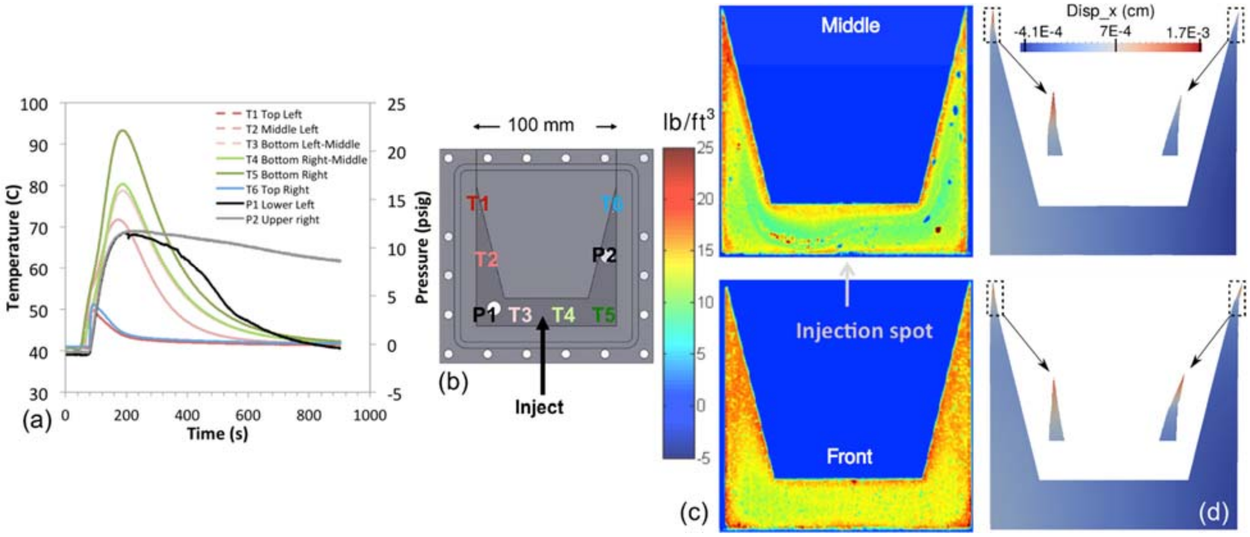

Figure 10.(a) Temperature and pressure profiles measured at the wall from locations in the staple mold geometry (a) showing locations of thermocouples (T), pressure transducers (P), and the injection port. Time is measured from the mixing time of the two components. (c) False color X-ray CT image of the density of a specimen halfway through the middle of the sample (into the page), showing many large bubbles in the arms and a high density skin near the walls. (d) Corresponding FEA showing the fully depressurized warped state along the middle and front slices. Note the distinct warpage at the tips between the two slices.

The dimensional change of a foamed specimen is measured at both the base and 80% of the distance to the tips. The dimensional change at each location is displayed in Figure 11 with respect to the aluminum mold width at the cure temperature of 120^{o}C. At the base, a large initial shrinkage of about 0.6% is observed at short times that is attributable to the thermal/cure contraction of the sample. Then, over approximately 14 days, a slow contraction is observed that adds an additional 0.1% shrinkage. This contraction diminishes over time until it is approximately equal to the error in the measurement. The width of the staple at the arms of the specimen follow an unpredictable, unsteady movement. This movement could be due to the anomalous large bubbles contained within the arm or some other unknown factor. Previous experiments from Atomic Weapons Establishment have shown transient motion in the staple tips showing a waving motion over long times [Pockett and Warriner, 2013].

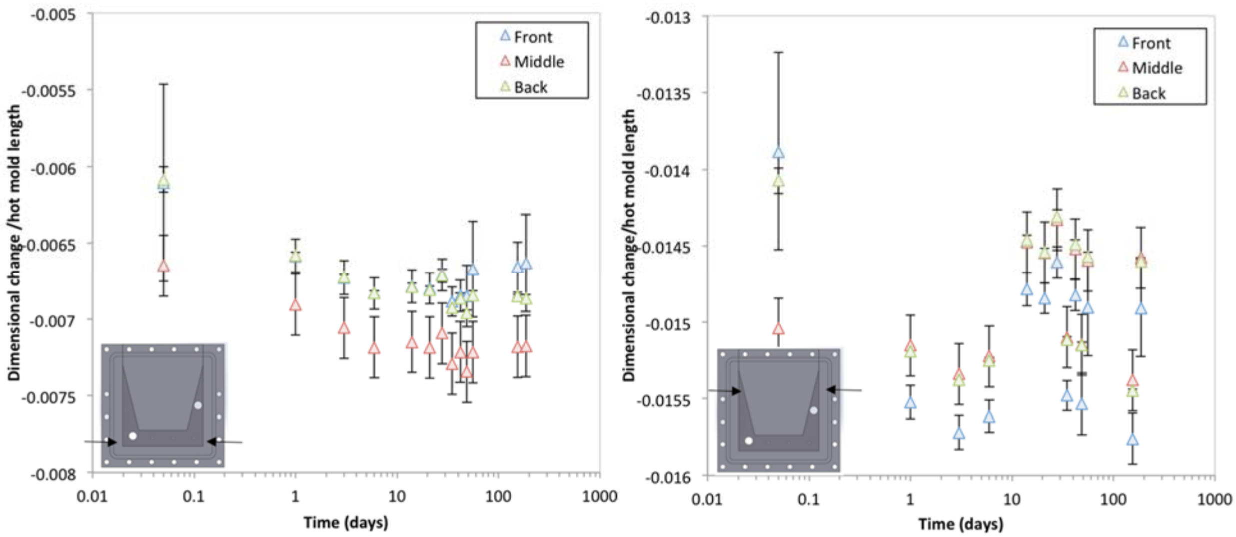

Figure 11. Staple width dimensional change normalized by the predicted mold width at the curing temperature (120°C) for (left) the base of the staple and (right) 80% up the staple arms. Front, middle, and back refer to the location of the trace in the depth of the mold (into the page as pictured)

The staple simulations show in Figure 10, only include the depressurization effects on the foam from its final density and do not include the shape change from the thermal/cure stresses during molding. If we go back and include both effects, we actually over-predict the size change from depressurization (Figure 12).

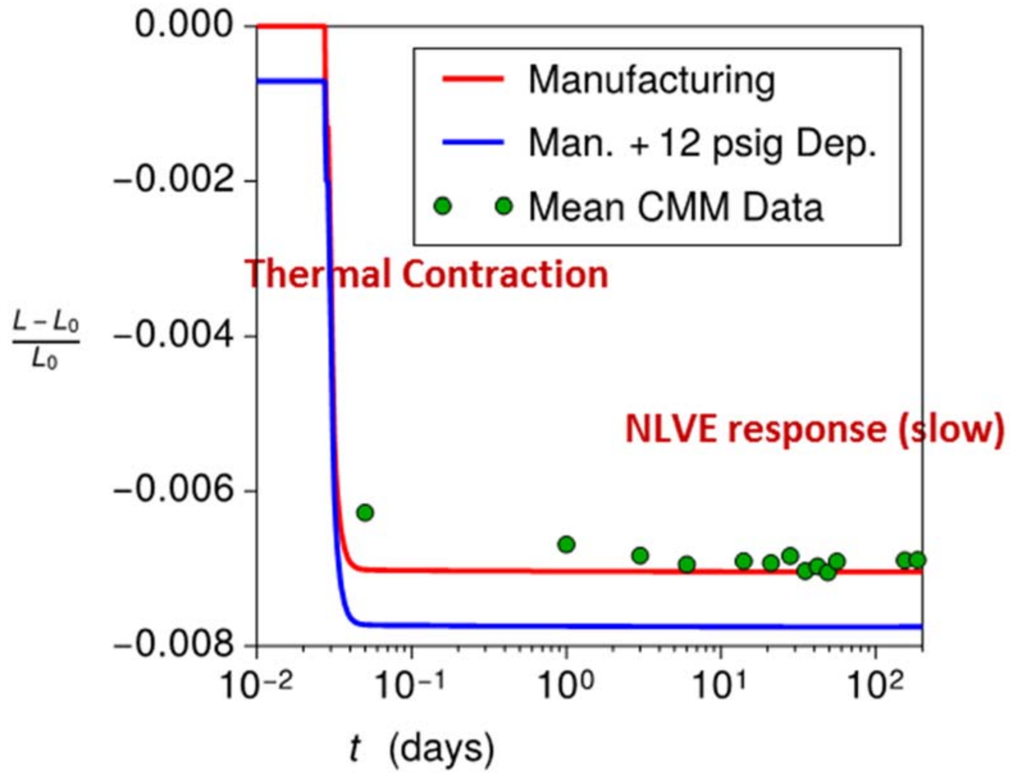

Figure 12. Staple shape change at the waist of the part showing data (green dots) compared to the NLVE response (red line) from molding to 100 days. The maximum depressurization strain for 12 psig initial pressure is added to the NLVE repsonse to show the direction of the solid response(blue line).

From Figure 12, we can see that the NLVE response for the staple slightly over-predicts the thermal/cure shrinkage and possibly grossly over-predicts the depressurization strains.

We decided to step back from the staple and look at a simpler geometry, which was a set of cylinders molded for different densities and formulations. These cylinders were measured with CMM until they reached their final size. We then did some careful work evaluating the three different depressurization models: analytical in Python, semi-analytical homogenized in Sierra Mechanics, and mesoscale with RVE simulations in Sierra. All three methods gave reasonably similar results as seen in Figure 13.

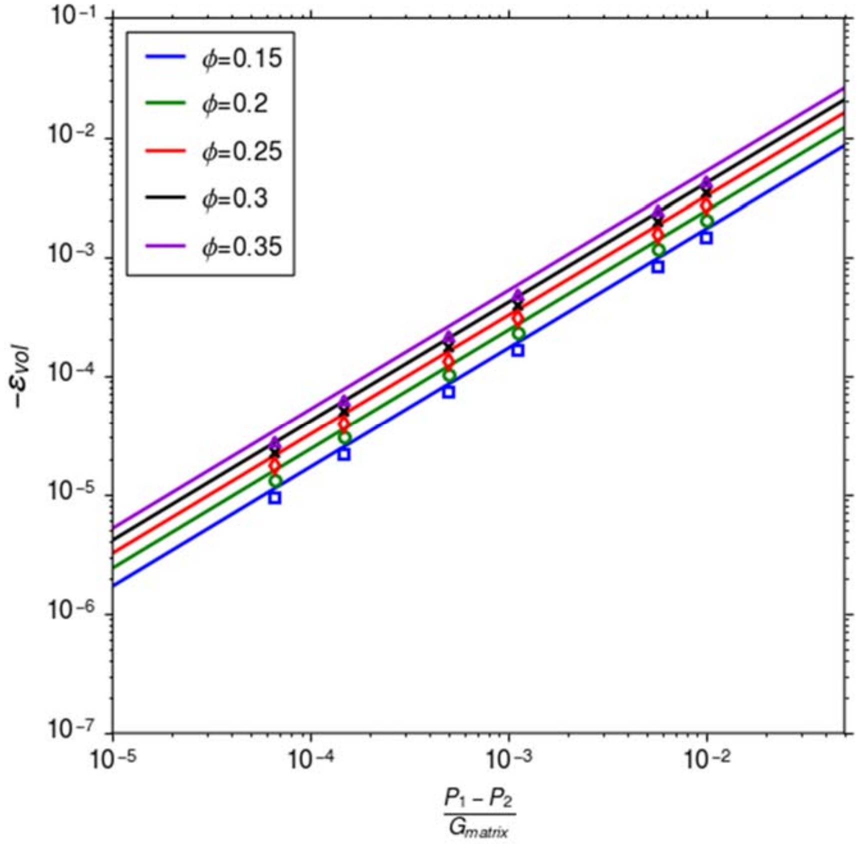

Figure 13. Comparison of analytic model predictions and micromechanics simulation results. The markers indicate the micromechanics results.

Using the Python version of the model and our best estimates for properties:

- All water is converted to CO_2 and allowed to pressurize the bubbles. This ignores the gas dissolved in the solid polymer, which could be up to 2-4% by weight.
- 0.174 mol CO_2 per kg resin (S10)
- 0.473 mol CO_2 per kg resin (E4)
- 0.0655 mol CO_2 per kg resin (E18)
- Glassy Shear Modulus = 570 MPa, Poisson Ratio = 0.4
- Foaming and Gelation Temperature of 40^oC
- Ideal Gas Assumption for CO_2 and air flow back into the foam
- 84 kPa air pressure at ambient (5000 Feet)
- Solid density of PU = 1100 kg / cubic meters
- Foams of uniform density

We get the following pressure and strain as a function of foam density, assuming the formulation is the same across the density map (Figure 14).

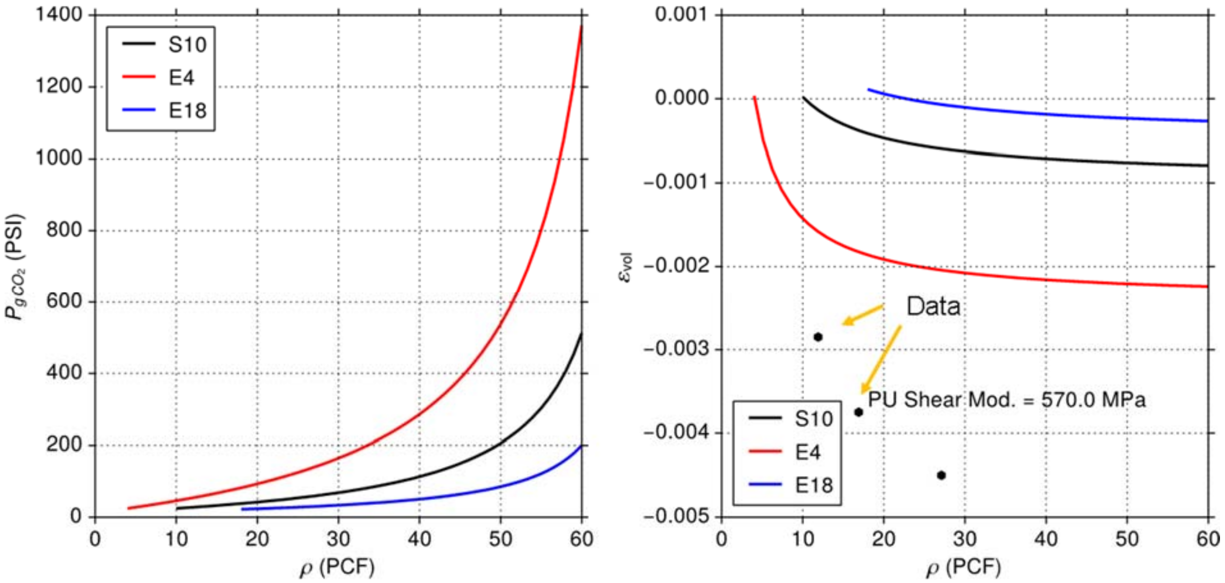

Figure 14. Base Case for pressure of carbon dioxide and shrinkage for depressurization assuming the properties given above.

If we assume that we have double the amount of water than is in the formulation and that the shear modulus is roughly 3 times smaller, we get an adequate match to data (Figure 15). However, a shear modulus of 177 MPa seems very unlikely for a glassy polymer.

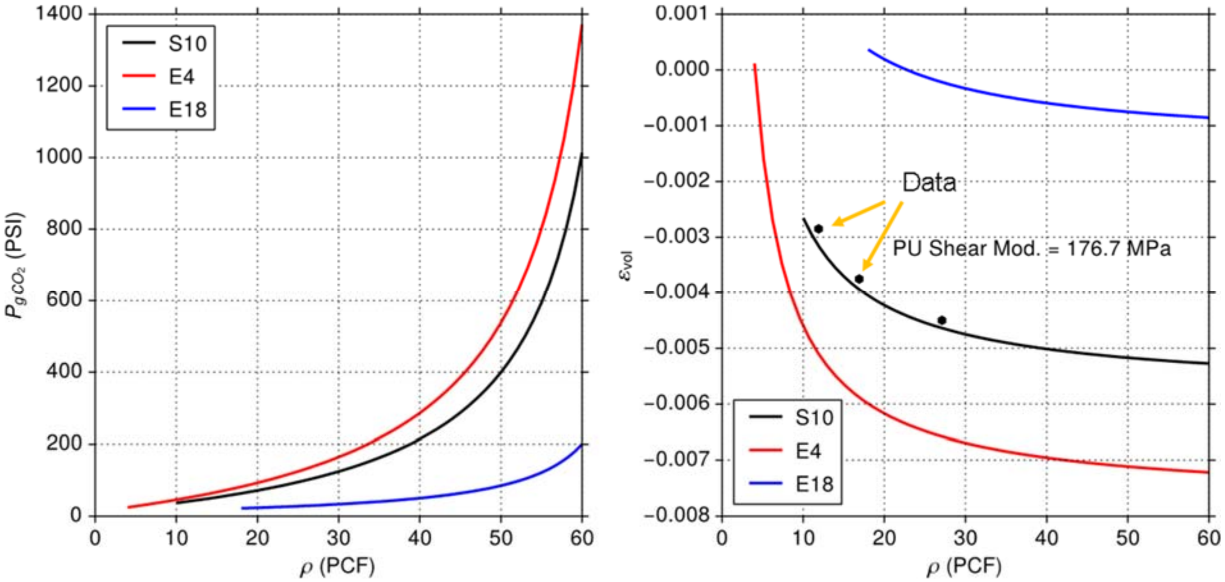

Figure 15. Modification of analysis using twice as much water and a very soft shear modulus (176.7 MPa). Results show the right shape of the cure and match well with the data. However, such a small value of the shear modulus seems unrealistic for a glassy polymer.

From this careful study of the depressurization shape changes over time, we have concluded that depressurization alone is not enough to account for our long-term post-manufacture shrinkage. As we looked for an additional mechanism, we recalled the confusing data of the samples held at 30°C that gained weight instead of losing weight. We realized that PMDI is hygroscopic and has been known to swell when exposed to a humid environment. This will cause a net gain weight, because the water will be absorbed into the foam (Figure 16).

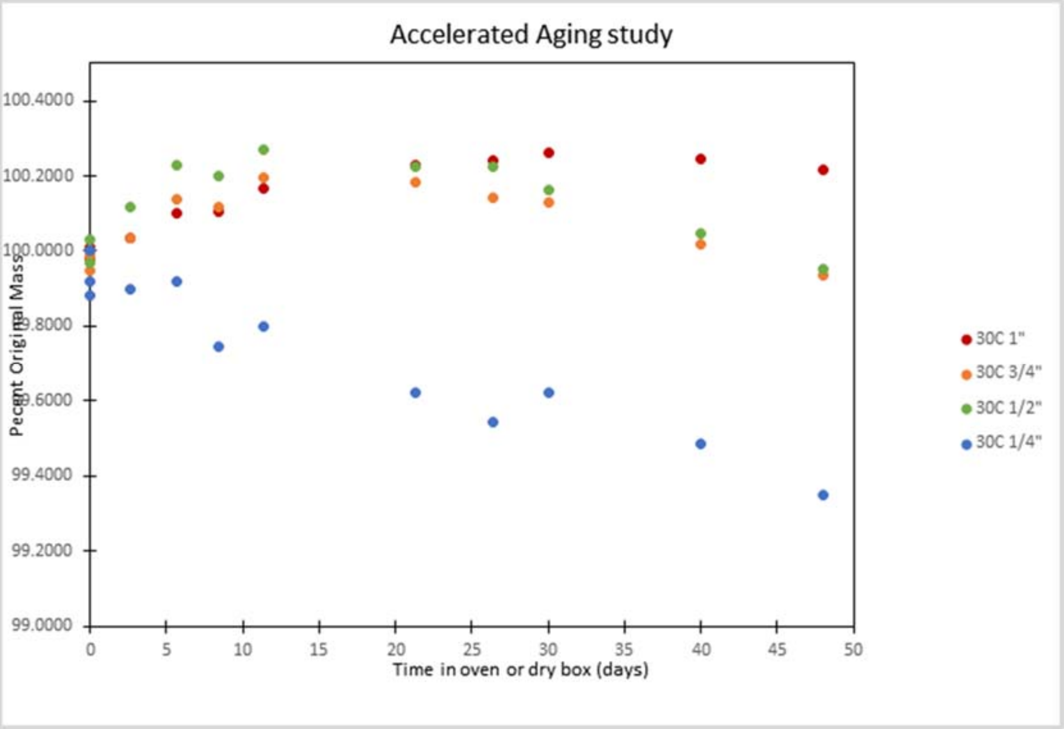

Figure 16. Foam bars held at 30°C experience ambient lab conditions, including high humidity. It was found that samples of different sizes experience different time-scales. Most samples showed initial mass gain and then subsequent mass loss, though the thinnest 1/4in samples look to have a very quick mass gain period that is missed in this experiment.

In addition, the stoichiometry of the PMDI-10 structural foam means that there is a lot of unreacted isocyanate available to react with the water. We think both water uptake and post-cure reactions are occurring and we are trying to quantify shape changes for these additional two effects. Our foam will swell with the water and gain weight. Subsequently, it loses weight. We have decided that the water reacts to form CO_2 which then escapes, leading to this transient effect. The water uptake is fast, but then it must diffuse to an isocyanate group to react, so there is time dependence. Once reacted, the CO_2 reaction product must diffuse back out, which leads to another transient time scale. In addition, it has been seen experimentally that water diffusion in polyurethane foam is two orders of magnitude faster than CO_2 diffusion [Rietz, 1983]. This can lead to complicated behavior for foams where the mass is a function of time and both mass gain and swelling and mass loss and shrinking are seen.

Conclusions, Impacts, and Future Work

We have measured the dimensional change of a chemically blown PMDI 13 lb/ft^3 foam over the course of 200 days, and these measurements show that, despite large defects within the foam from processing, overall shrinkage is more uniform in thick regions than in thin regions. Accompanying FEA simulations using a constitutive model based on a simple micromechanics model of foam depressurization corroborates this finding. We note that under uniform density/gauge pressure conditions, the model is analytic, and it shows a direct trade-offs between gauge pressure, foam porosity, and volume change due to depressurization.

Our model has improved greatly since last year but still faces challenges to allow for quantitative predictions of shape change out of the mold and over time. We believe a model is necessary to be able to design age-aware molds that are can handle shape change due to cure/thermal shrinkage during manufacture, as well as all three now identified aging mechanisms: depressurization, water uptake, and excess isocyanate reactivity. Sadly, just as we have made this discovery, our project ran out of ES funding.

Summary of Findings and Capabilities Related to Aging

Through a combination of modeling and experiment, we believe we have determined the most important mechanisms for shape change in polyurethane foamed part during manufacture and over time.

1. Thermal and cure stresses cause shrinkage once the part is released from the mold, and this is the largest shape change seen during the lifetime of the part.
2. Three aging mechanisms have been observed, which also lead to shape change.
   a. Bubble depressurization, which shrinks the foam part over its first year in the stockpile as the over-packed foam loses the gases in the bubbles, which have a pressure higher than ambient. This will also lead to mass loss.
   b. Post-curing reaction of isocyanate with water, which also leads to mass loss and foam shrinkage.
   c. Water absorption, which can lead to swelling and weight gain in foam parts. If no free isocyanate exists, this effect should be reversible once the foam sees a dry environment.

We are currently working to model all dimensional instabilities for the B61 support molds. However, this work is also applicable to other systems such as W76-1, W78, W87, W88, and W80. We believe a model is necessary to be able to design age-aware molds that are can handle all these mechanisms of shape change.

Acknowledgments

The authors would like to thank the Sierra Aria team, especially David Noble, Sam Subia, and Scott Roberts, for help with the code coupling, and the Sierra/SM team for help with solution control. The authors have had helpful discussions with the entire focused exchange team about polyurethane foams and with Bob Chambers about the curing viscoelastic formalism and Jamie Kropka, Mat Celina and Anne Grillet about experiments to parameterize it. This project leveraged funding and previous work from a variety of sources including ASC, WSEAT, B61, and LDRD.

References, Publications, and Presentations

R. R. Rao, L. A. Mondy, D. Noble, V. Brunini, J. Tinsley, C. C. Roberts, K. Long, M. Soehnel, M. Celina, N. Wyatt, and K. Thompson. A Kinetic Approach to Modeling the Manufacture of High Density Polyurethane Structural Foam: Foaming and Polymerization. *SAND2015-8282*, Sandia National Laboratories, September 2015.

R. R. Rao, L. A. Mondy, K. Long, M. Celina, C. C. Roberts, M. Soehnel, N. Wyatt, and V. Brunini. The kinetics of polyurethane structural foam formation: foaming and polymerizations. *AIChE J.* (in review, 2016).

Long, K.N., Roberts, C.C., Soehnel, M.M., Mondy, L.A., Johnson, K., Rao, R.R., "Depressurization and Warpage in Fast Curing, Glassy PMDI Foams," SAND2016-3234 C, Polymer Processing Society 32, Lyon, France, 07/25/2016 - 07/29/2016

Long, K.N., Roberts, C.C., Soehnel, M.M., Mondy, L.A., Johnson, K., Deng, H., Stavig, M., Celina, M.C, Rao, R.R., "Cradle-to-Grave Modeling of Structural Foams: Nonlinear Viscoelastic Response During Manufacturing and Aging, in preparation, October, 2016b, SAND2016-????

Pockett, K. and Warriner, C., *Understanding the dimensional stability of rigid polyurethane foam*, AWE Report 283/13, 2013.

Rao, R.R., Mondy, L.A., Roberts, C.C., Soehnel, M.M., Long, K.N., Brunini, V.E., Noble, D. R., Voskuilen, T., Celina, M.C., "The fluid mechanics of polyurethane foam expansion and polymerization," Extended Abstract, SAND2016-0566 C, XXIV International Congress on Theoretical and Applied Mechanics, Montreal, Canada, 08/21/2016 - 08/26/2016

Reitz, D.W., "A Basic Study of Gas Diffusion in Foam Insulation," Master's Thesis, MIT, 1983.

Administrative Addendum

Related Publications and Presentations:

1. Rao, R.R., Long, K.N., Mondy, L.A., Roberts, C.C., Soehnel, M.M., Johnson, K., Brunini, V.E., Noble, D. R., Voskuilen, T., "Including Bubble-Scale Information in Continuum Foam Expansion And Aging Models" SAND2016-8089 PE, ***Invited Presentation***, Workshop on Mathematics for Mesoscopic Modeling of Materials, Albuquerque, NM, 08/30/2016 - 08/31/2016
2. Rao, R.R., Mondy, L.A., Roberts, C.C., Soehnel, M.M., Long, K.N., Brunini, V.E., Noble, D. R., Voskuilen, T., Celina, M.C., "The fluid mechanics of polyurethane foam expansion and

polymerization" ***Invited Keynote,*** SAND2016-8010 C, XXIV International Congress on Theoretical and Applied Mechanics, Montreal, Canada, 08/21/2016 - 08/26/2016

Milestone Status:

Re-parameterize kinetic model for curing reactions based on improved IR data. Identify other areas of improvement necessary to capture post-gelation kinetics including vitrification for solid stresses.	Q1	We have completed this milestone and include results in a Journal Article report [Rao et al., 2016].
Develop validated foam filling model for horseshoe geometry using flow visualization data to provide initial conditions for nonlinear viscoelastic stress model	Q2	We have completed this milestone and include results in a presentation to ES and PPS [Long et al., 2016]
Develop model for foam filling, cure, and aging of foam in pop-off tube geometry. Measure evolving modulus during polymerization for dry polyurethane using a rheometer and DMA.	Q3	We have completed this milestone and are compiling the results in a forthcoming SAND report [Long et al., 2016b].
Validate shrinkage and stress relaxation model for horseshoe geometry against experimental data.	Q4	We have completed this milestone and include results in this report.

- **Financial Leveraging:**

The work represented was paid for by:

Source	**Dollar Amount ($k)**
Enhanced Surveillance	100K
ASC	100K
Systems (B61)	50K

Acronym/Abbreviation List

[Acronym]	[Meaning]